Microchimica Acta (2020) 187:493
https://doi.org/10.1007/s00604-020-04469-3

ORIGINAL PAPER

Coating silver metal-organic frameworks onto nitrogen-doped porous carbons for the electrochemical sensing of cysteine

Xiurong Zhai[1,2] · Shuai Li[2] · Xi Chen[3] · Yue Hua[2] · Hua Wang[2]

Received: 23 April 2020 / Accepted: 27 July 2020

Abstract

Nitrogen-doped porous carbons (N-PC) were coated for the first time with silver metal-organic frameworks (Ag-MOF) by the hydrothermal route. The resulted N-PC@Ag-MOF composites present high stability because of the strong interaction between N atoms of N-PC and Ag^+ ions of Ag-MOF. It was discovered that the electrodes modified with N-PC@Ag-MOF composites display much higher conductivity than the one modified with Ag-MOF. Especially, they provide stable and sharp electrochemical signals of solid-state AgBr at a low potential approaching zero (i.e., 0.02 V), which may aid to overcome the drawback of the traditional electroanalysis at high overpotentials with serious interferences from the samples background. More importantly, the yielded AgBr signals selectively decrease induced by cysteine (Cys) through the specific thiol-bromine replacement reactions that transfer AgBr into non-electroactive Ag-Cys. The proposed method facilitates the selective detection of Cys with two linear working ranges of 0.10 to 100 μM and 100 to 1300 μM, respectively. The N-PC@Ag-MOF-based sensors have been used for detection of spiked Cys in milk samples with good recovery efficiencies. The developed electroanalysis strategy for probing Cys through the specific thiol-bromine replacement has potential applications in the food analysis fields.

Keywords Electroanalysis · Cysteine · Ag-MOF · Nitrogen-doped porous carbons

Introduction

Cysteine (2-amino-3-sulphydrylpropanoic acid) (Cys), an essential amino acid containing thiol group, may exist in some daily foods (i.e., milk) as the high nutritional content [1–3]. It can also act as the physiological regulator for various diseases such as heart disease, rheumatoid arthritis, and AIDS [4]. Hence, the selective and sensitive detection of Cys levels in a variety of food products like milk is of great significance. Up to date, several analytical methods have been reported for the determination of Cys, such as the high performance liquid chromatography [5], fluorescence spectroscopy [6], flow injection [7], colorimetry [8], chemiluminescence [9], and electrochemistry analysis [10]. Among them, the electrochemical analysis is one of the most frequently used and attractive analysis methods because of the inherent advantages of simplicity, easy miniaturization, high sensitivity, rapidity, and lower experimental costs. However, most of the electrochemical determinations for Cys with the modified electrodes may mainly performed by the electrochemical oxidation of thiol-containing Cys usually at the high overpotentials, leading to the low detection selectivity especially for the Cys in the complicated samples [11, 12].

Porous carbons (PC) as the versatile materials have attracted intensive attentions for the electrochemical catalysis applications [13, 14]. It is worth noting that the physical properties of PC can be efficiently adjusted by doping some heteroatoms like nitrogen (N) that may enter into the carbon frameworks to enable the redistribution of their overall

Electronic supplementary material The online version of this article (https://doi.org/10.1007/s00604-020-04469-3) contains supplementary material, which is available to authorized users.

✉ Hua Wang
huawang@qfnu.edu.cn

[1] Department of Chemistry and Chemical Engineering, Jining University, Qufu City 273155, Shandong Province, People's Republic of China

[2] Institute of Medicine and Materials Applied Technologies, School of Chemistry and Chemical Engineering, Qufu Normal University, Qufu City 273165, Shandong Province, People's Republic of China

[3] Chemistry and Chemical Engineering, Harbin Institute of Technology, Harbin City, Heilongjiang Province, People's Republic of China

Published online: 08 August 2020

electron density [15, 16]. As a result, the electrochemical catalytic performances of the N-doped PC (N-PC) materials can be recognized by N doping to promise for the improved applications for the chemical sensors and biosensors [17–19]. Also, they can attain the better multifaceted features such as large surface area, unique pore structure, good electrochemical stability and conductivity, excellent thermal and mechanical stability, and easy regeneration, compared with the pristine carbon materials [13–19]. For example, the N-PC-modified electrodes were reported to possess the higher reaction activity for the electrochemical catalytic reduction of nitrobenzene to aniline [17]. The electrochemical biosensors were developed with co-embedded N-PC composites for sensitively probing H_2O_2 [18]. Also, the CuCo-coated N-PC materials were modified on the electrodes achieving the highly sensitive electrochemical analysis for luteolin [19].

Moreover, metal-organic frameworks (MOF) have received considerable interests due to their outstanding properties including high porosity, large surface area, and structural and chemical tunability [20]. However, most of the pristine MOF may currently suffer from the low conductivity, showing very limited electrochemical applications [21, 22]. Alternatively, many studies have been focused on the design of the MOF-based composites with suitable hybrid structure [23, 24]. For example, Ni-MOF was in situ synthesized on the graphene/Ni foam with the self-supporting hybrid structure for the all-solid-state supercapacitors with high energy density [23]. MOF/reduced graphene oxide composites were prepared by the electrostatic self-assembly method, showing the high electrical conductivity and excellent flexibility and mechanical properties [24]. Ag-based porous MOF (ZIF-67) fabricated and exhibited excellent electrocatalytic performances for glucose oxidation with high sensitivity and good selectivity and stability [25]. Ag-MOF were prepared by Ag(I) ions coordinated to oxygen groups in an organic ligand and could exhibit high electrocatalytic activity for the oxygen reduction reaction when they are incorporated in a porous carbon support [26].

In the present work, N-PC materials were firstly coated with silver (Ag) MOF to yield the N-PC@Ag-MOF composites by the hydrothermal method. It was discovered that in addition to the greatly improved conductivity, the N-PC@Ag-MOF-modified electrodes could display stable electrochemical oxidation peaks of AgBr at a lower potential near zero, which is helpful to overcome the defects of the traditional electroanalysis at high overpotentials with serious background interferences. Importantly, the highly specific responses to Cys could be thus achieved through the irreversible thiol-bromine replacement reactions resulting from the conversion of AgBr into non-electroactive Ag-Cys, showing the rational decrease in AgBr signals. Subsequently, the practical electroanalysis of Cys in milk was demonstrated with the favorable recovery efficiencies.

Experimental section

Reagents

$AgNO_3$, dicyandiamid (DCDA), 1,3,5-trimesic acid (H_3BTC), imidazole, acetonitrile, and tetramethyl ammonium hydroxide were all purchased from Sangon Biotech Co., Ltd. (China). Cysteine (Cys), phenylalanine (Phe), tryptophane (Try), leucine (Leu), lysine (Lys), methionine (Met), isoleucine (Iso), valine (Val), tyrosine (Tyr), glucose (Glu), saccharose (Sac), dopamine (DA), and ascorbic acid (AA) were purchased from Sigma-Aldrich (Shanghai, China). Phosphate buffer solution (1/15 M, pH 7.0) was used as the buffer solution. All chemicals reagents were of analytical grade. Double-distilled water was used throughout the experiments.

Apparatus

Scanning electron microscopy (SEM, Hitachi E-1010, Japan) and power X-ray diffraction (XRD, Xcalibur E diffractometer) were utilized for the characterization of the prepared composites. All the electrochemical experiments were characterized on the electrochemical workstation CHI 760E (CH Instrument, Shanghai, China). A conventional three-electrode system was applied consisting of glass carbon electrode (3 mm in diameter) as working electrode, which was polished firstly with alumina powder and then ultrasonically cleaned with water and alcohol, Pt wire as counter, and Ag/AgCl/3 M KCl as reference electrode. All experiments were performed at room temperature.

Synthesis of the N-PC@Ag-MOF composites

PC@Ag-MOF composites were prepared by the hydrothermal method. Firstly, the N-PC materials were synthesized according to the literature [27]. Briefly, MOF-5 was chosen as template, and DCDA was chosen as N precursors. The dried MOF was soaked in methanol solution in the presence of DCDA and carbonized at 900 °C in ultrapure nitrogen. Then, the obtained materials were washed with dilute hydrochloric acid solution and double-distilled water. Secondly, an aliquot of N-PC suspension (0.0100 g/L) was introduced into $AgNO_3$ (0.01277 g/mL) to be mixed for 30 min under vigorous stirring and further transferred into the 25 mL Teflon-lined stainless steel autoclave. Thirdly, H_3BTC (0.0399 g), imidazole (0.0399 g), and acetonitrile (2.0 mL) were added into the mixture of pH 6.5, which was regulated with tetramethyl ammonium hydroxide. Finally, the mixture was stirred for 30 min until completely dispersed and then heated at 120 °C for 6 h. After cooling to room temperature, the products were centrifuged and washed by distilled water and ethanol each for three times. The obtained black powder N-PC@Ag-MOF

were dried in vacuum at 60 °C for 4 h and further stored in dark.

Preparation of the N-PC@Ag-MOF-modified electrodes

N-PC@Ag-MOF composites (0.0100 g/L) were dispersed into the 2.0% Nafion solution. An aliquot of 3.0 μL of the above N-PC@Ag-MOF was then dropped onto each of the glassy carbon electrodes to be air-dried for future usage. The linear sweep voltammetries (LSVs) were performed at the potentials ranging from − 0.30 to 0.60 V at a scanning rate of 100 mV/s.

Electroanalysis of Cys

Electrochemical measurements for Cys with the N-PC@Ag-MOF-modified electrodes were performed in the buffer solution containing 100 mM Br^- ions. Furthermore, an aliquot of Cys of different concentrations was separately introduced into the above buffer solution for the electrochemical measurements by linear scanning voltammetries (LSVs). Moreover, the control tests were conducted accordingly for some other common ions, small molecules, amino acids, and compounds, including Mg^{2+}, Ca^{2+}, Zn^{2+}, Na^+, PO_4^{3-}, CO_3^{2-}, Cl^-, Phe, Try, Leu, Lys, Met, Iso, Val, Tyr, Glu, AA, Suc, and DA.

Three samples of fresh milk were obtained from local supermarket (Jining City, China), which were separately spiked with Cys of known concentrations (i.e., 10 mM and 20 mM). Then, an aliquot of 50 μL milk samples was introduced into 5 mL of the optimal phosphate buffer (pH 7.0), containing100 mM Br^- for the electroanalysis according to the same procedure above. Furthermore, the concentrations of added Cys in the milk samples were obtained to calculate the recovery efficiencies according to the rationally decreased currents of LSV at the potential of oxidation peak.

Results and discussion

Main fabrication procedure of N-PC@Ag-MOF for the electroanalysis of Cys

The main fabrication procedure of N-PC@Ag-MOF composites for the electroanalysis of Cys is schematically illustrated in Scheme 1. Herein, N-PC materials were mixed with $AgNO_3$, so that N atoms of N-PC could strongly coordinate with Ag^+. Once H_3BTC and iminazole were introduced into the hydrothermal process, the N-PC@Ag-MOF composites could be thus formed. Afterwards, N-PC@Ag-MOF composites were modified on the electrodes, in which Ag^+ in N-PC@Ag-MOF composites would interact with Br^- ions in solution to form AgBr, showing the stable and sharp electrochemical signals of solid-state AgBr (Fig. S1). Further, when Cys was added, its −SH group would trigger the transferring of AgBr into Ag-Cys with no electroactivity by conducting the thiol-bromine replacement, because the Ag-Br interaction is much weaker than that of the Ag-Cys one. Therefore, a rational decrease was thus observed in the AgBr signals toward the electroanalysis of Cys by the signal output of solid-state Ag/AgBr electrochemistry.

Characterization of N-PC@Ag-MOF composites

Morphological studies of the N-PC and the developed N-PC@Ag-MOF composites are comparably carried out by SEM imaging (Fig. 1). One can note from Fig. 1a that N-PC could show the flat structure with many large pores of several hundred nanometers in size. Remarkably, the N-PC@Ag-MOF composites display similar sheet structures, which may prove the successful decoration of micro-sized Ag-MOF over N-PC layers (Fig. 1b). Also, the surface morphology of N-PC@Ag-MOF composites was studied by elemental mapping, with the data shown in Fig. S2. It was found that the elements of Ag, C, O, and N could be distributed homogeneously throughout the N-PC@Ag-MOF composites. Furthermore, the power XRD pattern was performed (Fig. S3). It was observed that N-PC@Ag-MOF composites could exhibit several peaks at diffraction angles (2θ) of 10.56°, 29.45°, 30.74°, 32.97°, and 40.13°, corresponding to the (020), (241), (225), (046), and (400) planes, respectively [28]. Therefore, these results indicate the successful formation of N-PC@Ag-MOF composites.

Figure 2 presents the cyclic voltammetries (CVs) of various modified electrodes in buffer solution. It can be seen that no obvious redox peaks could be observed for the N-PC-modified electrode. Also, the Ag-MOF-modified electrode could present the CV curve that was not smooth with some serrations (Fig. 2 inset). In contrast, the N-PC@Ag-MOF-modified electrode could display the highest current density with the smooth CV curve, because that N-PC containing in the N-PC@Ag-MOF composites with high conductivity could facilitate the improved electronic transmission. Besides, one pair of redox peaks could be clearly observed for both of the Ag-MOF and N-PC@Ag-MOF-modified electrodes, which might be attributed to the redox reaction of Ag [29].

Electrochemical Cys sensing properties for the N-PC@Ag-MOF-modified electrodes

The LSV curve of the Ag-MOF-modified electrode was considerably rough, and especially the signal was very small after adding Cys (Fig. S4). However, the N-PC@Ag-MOF-modified electrodes offered high current response for the electroanalysis of Cys through the solid-state Ag/AgBr

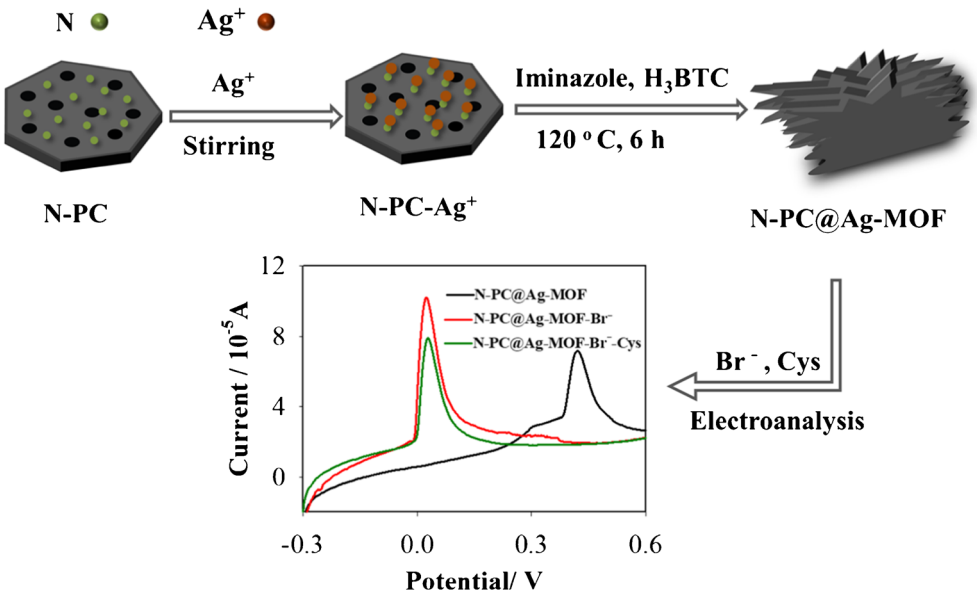

Scheme 1 Schematic illustration of the step-by-step synthesis procedure of N-PC@Ag-MOF composites and the electrochemical responses to Br^- ions and then Cys

electrochemistry. Figure 3 shows the characteristic electrochemical LSV responses of the N-PC@Ag-MOF-modified electrode to Cys without and with Br^- ions. It was found that after adding Br^- ions, the N-PC@Ag-MOF-modified electrode could present a large and stable AgBr oxidization peak current at the potential approaching zero (i.e., 0.02 V). More importantly, the addition of Cys could induce a great decrease in the AgBr current of the N-PC@Ag-MOF-modified electrode, which might circumvent the high overpotential disadvantages of traditional electrochemical oxidation of Cys.

The above effects might be explained by the following reasons. Although Ag^+ in Ag-MOF could interact with Br^- ions to form AgBr, the electrical conductivity of Ag-MOFs was too poor to cause high current responses after adding Cys. However, N-PC containing in N-PC@Ag-MOF composites could possess high conductivity to improve the electron transferring between Ag-MOFs and Br^- ions. As a result, the most effective current response of the N-PC@Ag-MOF-modified electrode to Cys could be expected.

Optimization of main conditions for the Cys electroanalysis

The effects of the main electroanalysis conditions on the electroanalysis performances of the N-PC@Ag-MOF-modified electrodes were investigated, including Br^- amounts, response time, N-PC amounts, and pH values (3.0–10.0) (Fig. S5). The effects of Br^- amounts on the electroanalysis performances of the Br-SH replacement were investigated. It was noted that the peak currents of solid-state AgBr could increase as the Br^- concentrations increase up to 100 mM, over which the current signal was almost unchanged (Fig. S5A). Accordingly, 100 mM Br^- ions were thereby chosen as the optimal one. Figure S5B exhibits that the reaction of Br-SH replacement could reach the equilibrium within 50 s, acting as the optimal response time. Moreover, it was found that the amounts of N-PC could significantly affect the current responses of the modified electrodes. The currents of AgBr could increase with increasing N-PC amounts until 1.0 mg/mL, over which the

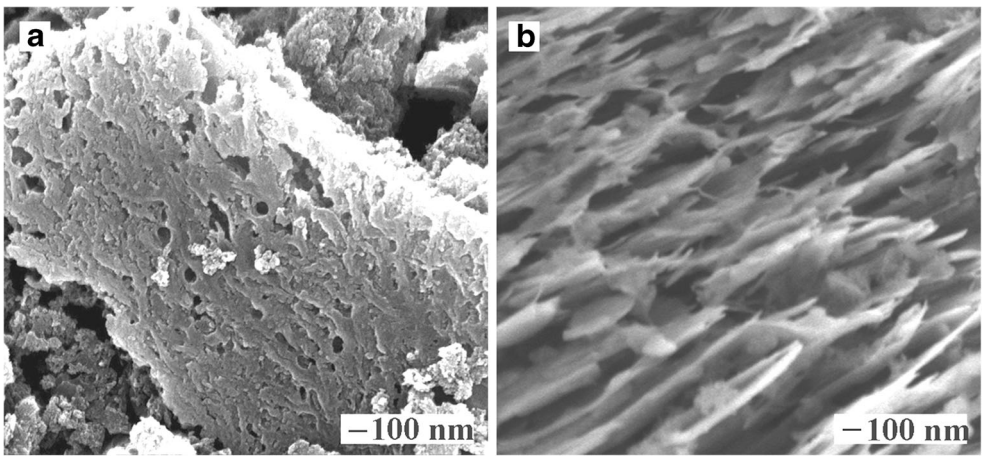

Fig. 1 SEM images of (**a**) N-PC and (**b**) N-PC@Ag-MOF composites

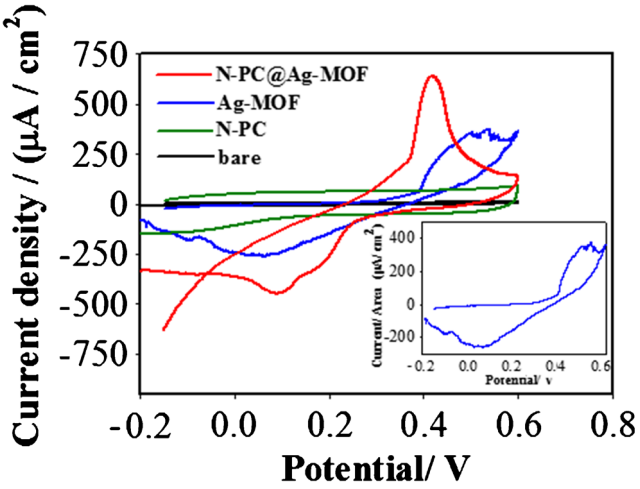

Fig. 2 Electrochemical CV characterization of the bare, N-PC, Ag-MOF, and N-PC@Ag-MOF-modified electrodes in the phosphate buffer solution (pH 7.0). Scan rate: 50 mV/s (inset: CVs of the Ag-MOF-modified electrode)

changed current signals were not obvious. The phenomenon may presumably be attributed to the fact that too high N-PC amount might lead to the low ratio of Ag content, so as to bring about the reduced chance of Br-SH replacement reactions (Fig. S5C). Accordingly, 1.0 mg/mL of N-PC was thought to be the optimal amount in the experiments. Also, the pH values could influence the electrochemical signals of Cys (Fig. S5D). Obviously, the highest current change could be obtained at pH 7.0, which should be selected as the suitable one.

Electroanalysis performances of the N-PC@Ag-MOF-based sensor for Cys

The selectivity of the N-PC@Ag-MOF-modified sensors for Cys electroanalysis was explored, in comparison with the common ions, small molecules, and amino acids with the same concentration (200 μM) possibly co-existing in milk

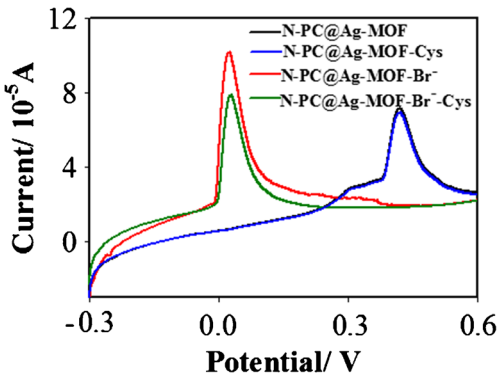

Fig. 3 Characteristic electrochemical LSV for Ag-MOF@N-PC-modified electrode before and after adding Br^- ions (100 mM) and then Cys (200 μM) in the phosphate buffer solution (pH 7.0). Scan rate: 100 mV/ s

(Fig. 4). As shown in Fig. 4a, by comparison, all of the other kinds of analytes tested could individually present the negligibly low responses. Importantly, when these substances possibly co-existing in milk were separately mixed with Cys, they could exert no significant effects on the Cys responses (Fig. 4b). Further investigations had been directed to detect 200 μM Cys in the presence of Try with the concentration of 20 mM, and no obvious interference was encountered for the determination of Cys (Fig. S6). Accordingly, this developed electroanalysis method with good anti-interference ability could selectively probe Cys in some complicated samples. These phenomena could be explained by the following reasons. The selective detection of Cys containing thiol groups could be realized through the transferring of AgBr into non-electroactive Ag-Cys product resulting from the specific thiol-bromine replacement reactions. However, the common ions, small molecules, and other amino acids could present no significant responses, because they do not contain thiol groups that can possess the stronger interaction with Ag^+ so as to conduct the thiol-bromine replacement reactions.

The reproducibility for sensing Cys was investigated using six N-PC@Ag-MOF-modified electrodes (Fig. S7A), showing the statistical standard deviation of about 4.4%. Meanwhile, electrochemical investigations were carried out on the storage stability of N-PC@Ag-MOF-modified electrodes (Fig. S7B). As expected, no obvious current changes were monitored for the tested electrodes modified with N-PC@Ag-MOF that were stored even up to 6 months. Besides, the N-PC@Ag-MOF-modified sensors were applied to detect Cys with the same concentrations (Fig. S8). Accordingly, the changes of Cys responses could present the high consistency, indicating that the modified electrodes might be reused for five cycles for the Cys with low concentrations (i.e., 10 μM). These results prove that the developed N-PC@Ag-MOF-modified electrodes could present high reproducibility and long-time stability for the detection of Cys.

Under the optimized conditions, the developed electroanalysis method was applied for sensing Cys with different concentrations (Fig. 5). As shown in Fig. 5a, it was found that with the increasing Cys concentrations, the current responses of the N-PC@Ag-MOF-modified electrodes decreased, and the potential of oxidation peak slightly shifted to the left because the potentials of oxidation peak might become smaller according to the Nernst equation ($E = {}^{Ag^+/Ag}E^{\theta}_{Ag^+/Ag} + \frac{RT}{F}\lg\frac{K_{sp}AgBr}{Br^-}$). Figure 5 b shows a linear relationship over Cys concentrations in the range from 0.10 to 100 μM and 100 to 1300 μM, with the changed current at the potential of oxidation peak (i.e., 0.02 V) with the scan rate of 100 mV/s. The limit of detection (LOD) is estimated to be 0.050 μM, based on signal-to-noise ratio of 3. Furthermore, the detection performances of the developed electroanalysis strategy are compared with those of the other electroanalysis

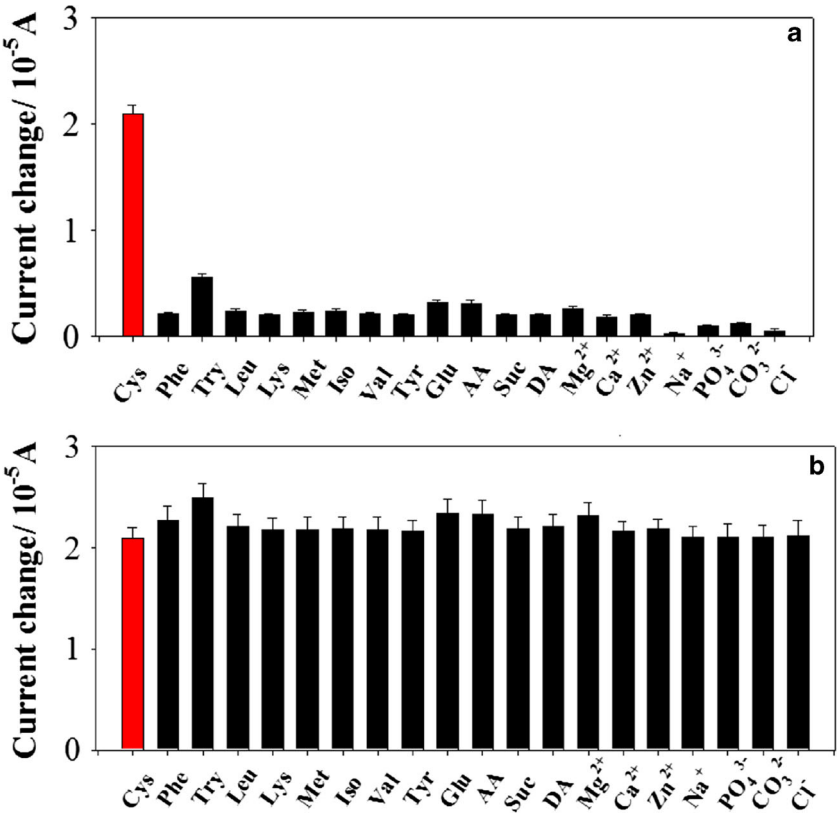

Fig. 4 Electrochemical LSV responses of the N-PC@Ag-MOF-modified electrode to (**a**) different interferents indicated alone and (**b**) interferents mixed separately with Cys at the same concentration (200 μM) at the potential of oxidation peak (i.e., 0.02 V) with the scan rate of 100 mV/s, in the phosphate buffer solution (pH 7.0)

methods for Cys reported previously, with the analysis results summarized in Table 1. It can be seen that the developed N-PC@Ag-MOF-modified electrodes could present better or considerable determination capabilities than the current electroanalysis methods for Cys in terms of the response overpotential, detection linear range, and LOD. Therefore, the developed electrochemical sensors may promise the sensing analysis of Cys in various samples.

Herein, the so developed N-PC@Ag-MOF composites are thought to play three kinds of main roles in the performances of electrochemical detections. Firstly, N-PC@Ag-MOF composites could present the high stability because of the strong interaction between N atoms of N-PC and Ag^+ ions of Ag-MOFs, which may enable the improved reproducibility of Cys electroanalysis. Secondly, the N-PC@Ag-MOF composites could enable the modified electrodes to display the sharp and stable responses of solid-state Ag/AgBr electrochemistry at a considerably low potential approaching zero (i.e., 0.02 V). Thirdly, the selective detection of Cys could be realized through the specific bromine-thiol replacement reactions that could transfer AgBr into non-electroactive Ag-Cys products.

Real sample analysis

Rapid and efficient analytical methods for the detection of Cys are significant in the analysis fields. Some reported methods have determined the concentration of Cys in practical samples

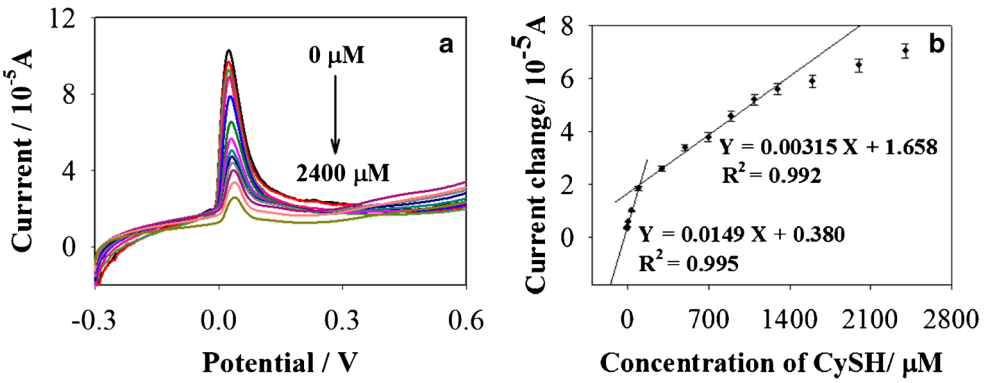

Fig. 5 (**a**) Electrochemical LSV responses to Cys of different concentrations in the phosphate buffer solution (pH 7.0), measured at a scan rate of 100 mV/s. (**b**) The calibration curve for the relationship between the changed currents of electrochemical LSVs at the potential of oxidation peak (i.e., 0.02 V) and the concentrations of Cys. Scan rate: 100 mV/s

Table 1 Comparison of the analytical results for Cys among different electroanalysis methods

Modifiers	Techniques	Overpotential (V)	Linear ranges (μM)	LOD (μM)	References
Ag-PDA/ITO	LSV	0.43	0.05–300	0.02	[30]
GR/CD/Pt/SPE	DPV	0.25	0.5–40, 40–170	0.12	[31]
SPE/PB-NH_2	Amperometry	0.87	100–500	72.0	[32]
CNF-M13	CV	0.40	20–1000	20.0	[33]
AuNPs/TrB/GCE	Amperometry	0.40	5.0–270.0	0.0060	[34]
RGO/4	Amperometry	0.50	5.0–47, 82–200	–	[35]
N-PC@Ag-MOF	LSV	0.02	0.10–100, 100–1300	0.050	Present work

[11, 36–38]. To examine the applicability and feasibility of N-PC@Ag-MOF-modified sensors, contents and recovery efficiencies of Cys in three milk samples were determined. Milk samples were diluted 100 times using phosphate buffer solution (pH 7.0). Table S1 summarizes the analytical results of different Cys levels in the milk samples, in which the recovery efficiencies were obtained ranging from 93.0 to 107.0%, indicating that these modified sensors should have the potential applications for the determination of Cys in real milk samples.

Conclusions

In summary, it was discovered that the electrodes modified with N-PC@Ag-MOF composites could display the sharp and stable responses of solid-state AgBr electrochemistry at a near zero potential. Also, the selective detection of Cys could be realized through the transferring of AgBr into non-electroactive Ag-Cys product because of the specific Br-SH replacement reactions, which might aid to circumvent the disadvantage of the traditional electroanalysis methods at high overpotentials, showing the more serious interferences from the samples backgrounds. More importantly, the N-PC@Ag-MOF-modified sensors could be applied to determine Cys quantitatively in milk samples with good recovery efficiencies. Therefore, the developed electrochemical sensor may find extensive applications for the electroanalysis of Cys in real samples. Yet, the analytical performances of the electrochemical sensors should be further improved with greater selectivity and higher electrochemical responses in the future.

Funding information This work is supported by the National Natural Science Foundation of China (No. 21675099) and Major Basic Research Program of Natural Science Foundation of Shandong Province (ZR2018ZC0129), PR China.

Compliance with ethical standards

Conflict of interest The authors declare that they have no conflicts of interest.

References

1. Kumar DR, Baynosa ML, Shim JJ (2019) Cu^{2+}-1,10-phenanthroline-5,6-dione@electrochemically reduced graphene oxide modified electrode for the electrocatalytic determination of L-cysteine. Sensors Actuators B Chem 293:107–114
2. Bai YH, Xu JJ, Chen HY (2009) Selective sensing of cysteine on manganese dioxide nanowires and chitosan modified glassy carbon electrode. Biosens Bioelectron 24:2985–2990
3. Wang J, Wang H, Hao Y, Yang S, Tian H, Sun B, Liu Y (2018) A novel reaction-based fluorescent probe for the detection of cysteine in milk and water samples. Food Chem 262:67–71
4. Vinod KV, Philip AS (2014) AuNP based selective colorimetric sensor for cysteine at a wide pH range: investigation of capping molecule structure on the colorimetric sensing and catalytic properties. RSC Adv 4:18467–18472
5. Zhang W, Li P, Geng Q, Duan Y, Guo M, Cao Y (2014) Simultaneous determination of glutathione, cysteine, homocysteine, and cysteinylglycine in biological fluids by ion-pairing high-performance liquid chromatography coupled with precolumn derivatization. J Agric Food Chem 62:5845–5852
6. Gong D, Tian Y, Yang C, Iqbal A, Wang Z, Liu W, Qin W, Zhu X, Guo H (2016) A fluorescence enhancement probe based on BODIPY for the discrimination of cysteine from homocysteine and glutathione. Biosens Bioelectron 85:178–183
7. Lau C, Qin X, Liang J, Lu J (2004) Determination of cysteine in a pharmaceutical formulation by flow injection analysis with a chemiluminescence detector. Anal Chim Acta 514:45–49
8. Ge S, Yan M, Lu J, Zhang M, Yu F, Yu J, Song X, Yu S (2012) Electrochemical biosensor based on graphene oxide–Au nanoclusters composites for l-cysteine analysis. Biosens Bioelectron 31:49–54
9. Sun J, Hu Z, Zhang S, Zhang X (2019) A novel chemiluminescent probe based on 1,2-dioxetane scaffold for imaging cysteine in living mice. ACS Sensors 4:87–92
10. Selvarajan S, Alluri NR, Chandrasekhar A, Kim SJ (2017) Direct detection of cysteine using functionalized $BaTiO_3$ nanoparticles film based self-powered biosensor. Biosens Bioelectron 91:203–210
11. Zhang L, Ning L, Zhang ZF, Li SB, Yan H, Pang HJ, Ma HY (2015) Fabrication and electrochemical determination of L-cysteine of a composite film based on V-substituted polyoxometalates and Au@2Ag core–shell nanoparticles. Sensors Actuators B Chem 221:28–36
12. Cao F, Dong Q, Li C, Kwak D, Huang Y, Song D, Lei Y (2018) Sensitive and selective electrochemical determination of L-cysteine based on cerium oxide nanofibers modified screen printed carbon electrode. Electroanalysis 30:1133–1139

13. Cui L, Wu J, Ju H (2014) Nitrogen-doped porous carbon derived from metal-organic gel for electrochemical analysis of heavy-metal ion. ACS Appl Mater Interfaces 6:16210–16216
14. Li C, Wang Y, Xiao N, Li H, Ji Y, Guo Z, Liu C, Qiu J (2019) Nitrogen-doped porous carbon from coal for high efficiency CO_2 electrocatalytic reduction. Carbon 151:46–52
15. Chen P, Wang LK, Wang G, Gao MR, Ge J, Yuan WJ, Shen YH, Xie AJ, Yu SH (2014) Nitrogen-doped nanoporous carbon nanosheets derived from plant biomass: an efficient catalyst for oxygen reduction reaction. Energy Environ Sci 7:4095–4103
16. Xiang Z, Cao D, Huang L, Shui J, Wang M, Dai L (2014) Nitrogen-doped holey graphitic carbon from 2D covalent organic polymers for oxygen reduction. Adv Mater 26:3315–3320
17. Zhao XY, Li AL, Quan X, Chen S, Yu HT, Zhang SS (2020) Efficient electrochemical reduction of nitrobenzene by nitrogen doped porous carbon. Chemosphere 238:124636
18. Wu Z, Sun LP, Zhou Z, Li Q, Huo LH, Zhao H (2018) Efficient nonenzymatic H_2O_2 biosensor based on ZIF-67 MOF derived Co nanoparticles embedded N-doped mesoporous carbon composites. Sensors Actuators B Chem 276:142–149
19. Feng X, Yin X, Bo X, Guo L (2019) An ultrasensitive luteolin sensor based on MOFs derived CuCo coated nitrogen-doped porous carbon polyhedron. Sens Actuators B 281:730–738
20. Kim KJ, Lu P, Culp JT, Ohodnicki PR (2018) Metal-organic framework thin film coated optical fiber sensors: a novel waveguide-based chemical sensing platform. ACS Sensors 3:386–394
21. Fleker O, Borenstein A, Lavi R, Benisvy L, Ruthstein S, Aurbach D (2016) Preparation and properties of metal organic framework/activated carbon composite materials. Langmuir 32:4935–4944
22. Sundriyal S, Kaur H, Bhardwaj SK, Mishra S, Kim KH, Deep A (2018) Metal-organic frameworks and their composites as efficient electrodes for supercapacitor applications. Coord Chem Rev 369: 15–38
23. Meng HM, Hu XX, Kong GZ, Yang C, Fu T, Li ZH, Zhang XB (2018) Aptamer-functionalized nanoscale metal-organic frameworks for targeted photodynamic therapy. Theranostics 8(16): 4332–4344
24. Cheng J, Chen S, Chen D, Dong L, Wang J, Zhang T, Jiao T, Liu B, Wang H, Kai JJ, Zhang D, Zheng G, Zhi L, Kang F, Zhang W (2018) Editable asymmetric all-solid-state supercapacitors based on high-strength, flexible, and programmable 2D-metal-organic framework/reduced graphene oxide self-assembled papers. J Mater Chem A 6:20254–20266
25. Meng W, Wen YY, Dai L, He ZX, Wang L (2018) A novel electrochemical sensor for glucose detection based on Ag@ZIF-67nanocomposite. Sensors Actuators B Chem 260:852–860
26. Guo HX, Zhang YH, Zheng ZS, Lin HB, Zhang Y (2017) Facile one-pot fabrication of Ag@MOF(Ag) nanocomposites for highly selective detection of 2,4,6-trinitrophenol in aqueous phase. Talanta 1701:146–151
27. Li JS, Li SL, Tang YJ, Li K, Zhou L, Kong N, Lan YQ, Bao JC, Dai ZH (2014) Heteroatoms ternary-doped porous carbons derived from MOFs as metal-free electrocatalysts for oxygen reduction reaction. Sci Rep 4:5130
28. Awaleh M, Badia A, Brisse F (2006) Influence of the anion on the structure of Bis(methylthio)methane supramolecular coordination complexes. Cryst Growth Des 2006:2674–2685
29. Linge JM, Erikson H, Kasikov A, Rähn M, Sammelselg V, Tammeveski K (2019) Oxygen reduction reaction on thin-film Ag electrodes in alkaline solution. Electrochim Acta 325:134922
30. Thota R, Ganesh V (2016) Simple and facile preparation of silver-polydopamine (Ag-PDA) core-shell nanoparticles for selective electrochemical detection of cysteine. RSC Adv 6:49578–49587.i
31. Singh M, Jaiswal N, Tiwari I, Foster CW, Banks CE (2018) A reduced graphene oxide-cyclodextrin-platinum nanocomposite modified screen printed electrode for the detection of cysteine. J Electroanal Chem 829:230–240
32. Bonacin JA, Dos Santos PL, Katic V, Foster CW, Banks CE (2018) Use of screen-printed electrodes modified by Prussian blue and analogues in sensing of cysteine. Electroanalysis 30:170–179
33. Szot-Karpińska K, Leśniewski A, Jönsson-Niedziółka M, Marken F, Niedziółka-Jönsson J (2019) Electrodes modified with bacteriophages and carbon nanofibres for cysteine detection. Sensors Actuators B Chem 287:78–85
34. Taei M, Hasanpour F, Habibollahi S, Shahidi L (2017) Simultaneous electrochemical sensing of cysteine, uric acid and tyrosine using a novel Au-nanoparticles/poly-Trypan Blue modified glassy carbon electrod. J Electroanal Chem 789:140–147
35. Koczorowski T, Rębiś T, Szczolko W, Antecka P, Teubert A, Milczarek G, Goslinski T (2019) Reduced graphene oxide/iron(II) porphyrazine hybrids on glassy carbon electrode for amperometric detection of NADH and L-cysteine. J Electroanal Chem 848: 113322
36. Liu XR, Dong LN, Wang LX, Xua H, Gao SM, Zhong LL, Zhang SX, Jiang TT (2019) 2-Aminopurine modified DNA probe for rapid and sensitive detection of L-cysteine. Talanta 202:520–525
37. Zhang L, Cai QY, Li J, Ge J, Wang JY, Dong ZZ, Li ZH (2015) A label-free method for detecting biothiols based on poly(thymine)-templated copper nanoparticles. Biosens Bioelectron 69:77–82
38. Liu HF, Sun YQ, Yang J, Hu YL, Yang R, Li ZH, Qu LB, Lin YH (2019) High performance fluorescence biosensing of cysteine in human serum with superior specificity based on carbon dots and cobalt-derived recognition. Sensors Actuators B Chem 280:62–68